Photonic Crystals: Thermoresponsive Shape-Memory Photonic Nanostructures (Advanced Optical Materials 6/2014)

ARTICLE *in* ADVANCED OPTICAL MATERIALS · JUNE 2014

Impact Factor: 4.06 · DOI: 10.1002/adom.201470035

4 AUTHORS, INCLUDING:

A. Blanco

Instituto de Ciencia de Materiales de Madrid

70 PUBLICATIONS **2,941** CITATIONS

Thermoresponsive Shape-Memory Photonic Nanostructures

André Espinha, María Concepción Serrano, Álvaro Blanco, and Cefe López*

Technological applications increasingly demand materials with sophisticated features and improved functionalities. In this context, multifunctional materials (MFMs) are especially attractive as they are often capable of responding to different physical, chemical and/or biological stimuli. A particularly useful property that has been incorporated into MFMs is the shape-memory effect (SME), which was first identified in a gold-cadmium alloy[1] and posteriorly discovered in polymers (the so-called shape-memory polymers, SMPs).[2,3] SMPs are able to switch from a temporary to a permanent shape in response to an external stimulus.[4] They represent a more efficient alternative, less expensive and easier to implement with high throughput, than conventional shape-memory alloys. Although heat is typically responsible for directly triggering SME,[5] recent advances have identified indirect mechanisms such as electrical stimulation[6] or alternating magnetic field excitation.[7] Interestingly, there are also reports describing heat-independent light-activated SME.[8,9] In terms of chemical composition, SMPs made of acrylamides,[10] caprolactones,[11] and polyurethanes[12] have been explored as stimuli-sensitive polymers with advanced functionalities.[13] They are suitable for applications as diverse as self-deployable sun-sails or microfoldable vehicles.[14,15]

Despite SMPs having been extensively explored in bulk form,[12] the investigation of the SME at the micro/nano scales is a very recent topic.[16] Furthermore, the use of SMPs for producing nanostructures with photonic functionality is still in its infancy. In general terms, photonic structures refer to patterned media with features in a typical size of the order of, or below, visible or near-infrared radiation wavelengths. These features translate into a modulation of the refractive index that causes a strong radiation/matter interaction and significantly affects the electromagnetic density of states. In this context, strategies for achieving periodic structures exhibiting SME are highly desirable, in order to develop novel MFMs and optical devices. Contrary to SMPs, elastomers have been more employed in photonics although almost exclusively to take advantage of their elastic properties. For instance, some reports have demonstrated their use in the fabrication of elastic transmission gratings or lenses with real time control of the periodicity or the focal length, respectively.[17] They have been applied to the preparation of compression sensitive inverse opals which allow the mechanical tuning of the photonic stopgap position.[18] Elastomers have also played a fundamental role for studying color tunable photonic crystals (PCs),[19,20] whose lattice parameter might be controlled by deformation (mechanochromic effect) or elastomer swelling.[21] An equivalent approach was proposed for the development of tunable phononic crystals.[22] Another active area of research concerns flexible systems implemented, for instance, as UV-filters[23] and light emitting diodes or displays.[24] The present work addresses the fabrication of periodic nanofeatures with SME by using a replica molding approach for imprinting a 2D photonic nanostructure on the surface of a shape-memory elastomer. Structural and optical characterization of the as-produced system allowed to demonstrate its shape-memory functionality for configuring the lattice parameter or erasing the nanopattern. This property might be very attractive, for example, for the development of reusable or self-healing photonic elements with adaptive properties.

Polydiolcitrates (PDCs), first described by Ameer and colleagues in 2004,[25] have been recently identified as thermoresponsive elastomers presenting SME.[26] However, as far as we know, their applicability in the accomplishment of photonic nanostructured systems has not been reported in the literature yet. The synthesized polyester networks were obtained upon: (1) increase of the mol ratio of hydroxyl to carboxyl groups in the reaction mixture (4:3 in hydroxyl-dominant PDCs versus 1:1 in the original ones) and (2) the use of a more hydrophobic diol (e.g., 1,12-dodecanediol, DD). These polymers include covalent netpoints responsible for the permanent shape and hydrophobic micro-domains (either pre-polymer or DD-rich domains) physically cross-linked by intermolecular hydrophobic interactions as switch structures to fix the temporary shape. To investigate the SME of these polymers for potential photonic applications, we followed the general procedure depicted in **Figure 1**. The first step consisted of the synthesis of the pre-polymer solution composed of DD and citric acid. ^{1}H nuclear magnetic resonance (^{1}H-NMR) confirmed the mol ratio expected for both components (1.5) and the beginning of the condensation reaction (e.g., multiplicity of peaks at 2.6–2.9 ppm) (see Supporting Information (SI), Figure S7). Nanopatterning of the elastomer surface was achieved by using an approach inspired in soft-lithography[27] and, more specifically, in replica molding (Figure 1a).[28,29] Briefly, the pre-polymer solution was spread over the template, in our case a colloidal monolayer composed of polystyrene (PS) spheres of 870 nm in diameter (d). After curing at 90 °C for 12 h, the resulting cross-linked polymer (PDDC-HD) was peeled off from the monolayer. When evaluating the cross-linking degree of the so-produced elastomer, a M_c value of 736 g mol^{-1} was obtained, in range with those previously reported for this type of polyesters.[26] During cross-linking, the surface of the

A. Espinha, Dr. M. C. Serrano, Dr. A. Blanco, Prof. C. López
Instituto de Ciencia de Materiales de Madrid (ICMM-CSIC)
Calle Sor Juana Inés de la Cruz, 3
Cantoblanco 28049, Madrid, Spain
E-mail: mslopezterradas@sescam.jccm.es

DOI: 10.1002/adom.201300532

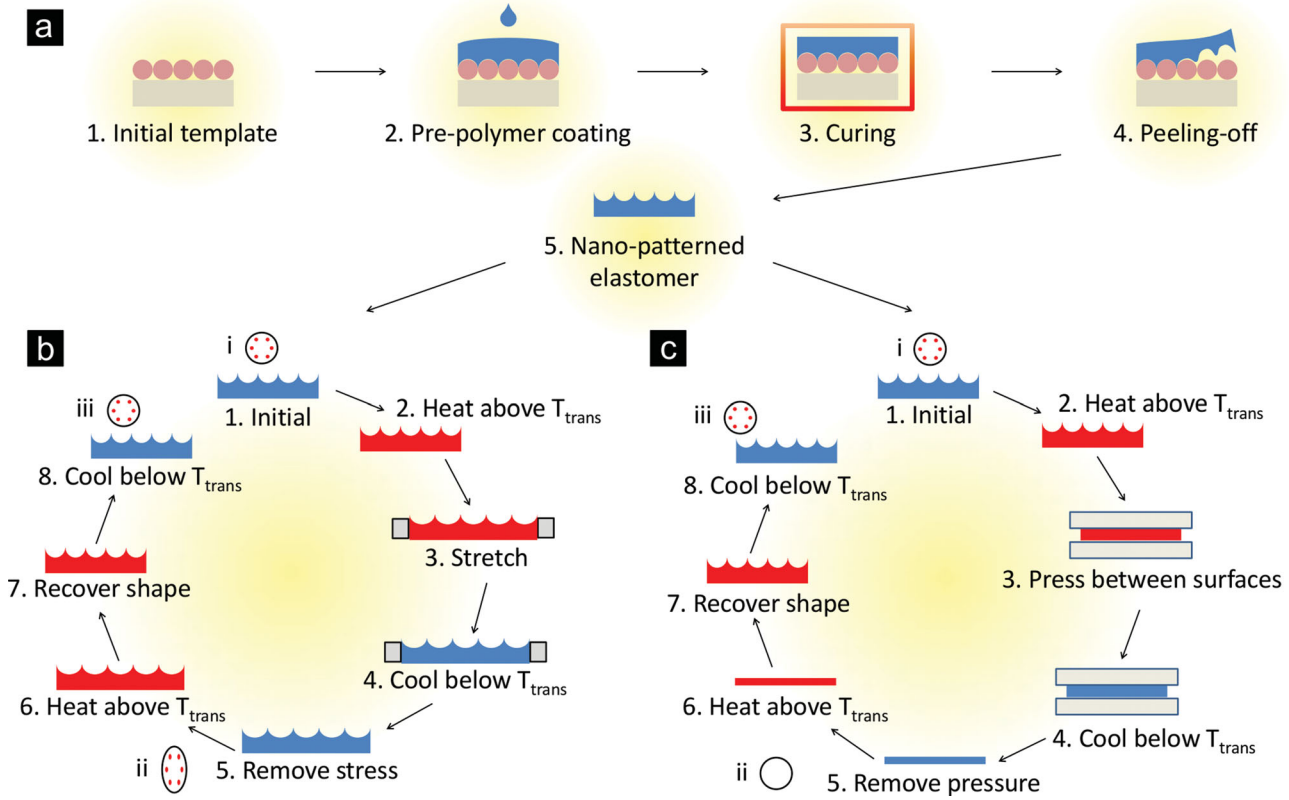

Figure 1. Scheme of the protocol followed for the grating imprint on the PDDC-HD elastomer surface (a) and study of its programmable shape-memory properties either varying the lattice parameter (b) or erasing the surface nanotopography (c).

PDDC-HD polymer acquired the permanent shape determined by the colloidal crystal structure, as confirmed by atomic force microscopy (AFM) studies (**Figure 2**). As can be observed, the elastomer surface consisted of a homogeneous hexagonal array of nanobowls of an average depth of 140 ± 30 nm. This surface nanopattern was created as a replica of the PS spheres monolayer, which remained in the mold after peeling off the cured polymer (Figure S1). This protocol was further confirmed suitable for templates composed of spheres with other diameters, as exemplified in Figure S2 for d = 200 nm. To avoid polymer cross-linking with the mold that could impair its removal, PS spheres were intentionally selected. By doing so, it was possible to peel off the cured elastomer from the template while still warm, to take advantage of its elastic properties. Additionally, the hydrophobic nature of the PS spheres contributed to repeal the elastomer from embedding deeply into the monolayer, thus explaining why the groove's depth obtained was on the order of 140 nm instead of the expected 435 nm, should the elastomer have reached at least the equator of the spheres.

Similarly to original PDDC-HD elastomers,[26] surface-nanopatterned PDDC-HD displayed both a glass transition at ca. –4 °C and a melting thermal transition responsible for the SME at ca. 30 °C, as revealed in the thermograms obtained by modulated differential scanning calorimetry (mDSC) (Figure S8). Above T_{trans} the polymer becomes an elastomer (rubber state) in which the degree of cross-linking and hydrogen bonding controls the elasticity of the network. Dynamic mechanical analysis (DMA) further confirmed the existence of these two transitions at a similar range of temperatures. Young modulus values of ca. 100 MPa were measured at 10 °C ($T < T_{trans}$) and 2 MPa above T_{trans} (e.g., 35 °C) (Figure S9). Interestingly, this transition could be monitored additionally via the optical properties of the polymer. The opaqueness characteristic of its glassy state at low temperature, caused by the scattering of light from the solid non-cross-linked micro-domains of pre-polymer and DD, gradually disappears as the material transits to the rubbery state. In this state, the micro-domains melt giving rise to a significant increase in transparency. This effect is exhibited in **Figure 3**, which presents the visual aspect of the sample at both room temperature (Figure 3a) and above T_{trans} (Figure 3b). We further explored this thermally-induced phenomenon by total optical transmittance spectroscopy measurements (Figure S3). A small disk of PDDC-HD (2.5 mm-thick) was heated at 90 °C for 10 min and then allowed to cool down at its natural pace while monitoring simultaneously the temperature and the total transmittance. Results for the wavelengths λ = 532 and 633 nm are presented in Figure 3c. From 70 °C to 26 °C, a constant plateau in which the transmittance was on the order of 95% was observed. As the temperature decreased below 26 °C, the transition was confirmed by a decrease in transmittance of ca. 70% (final sample transmittance 25–31%). This property is of considerable interest since it supports the applicability of PDDC-HD as a thermo-optical trigger (i.e., a device that transmits light only above a particular temperature threshold).

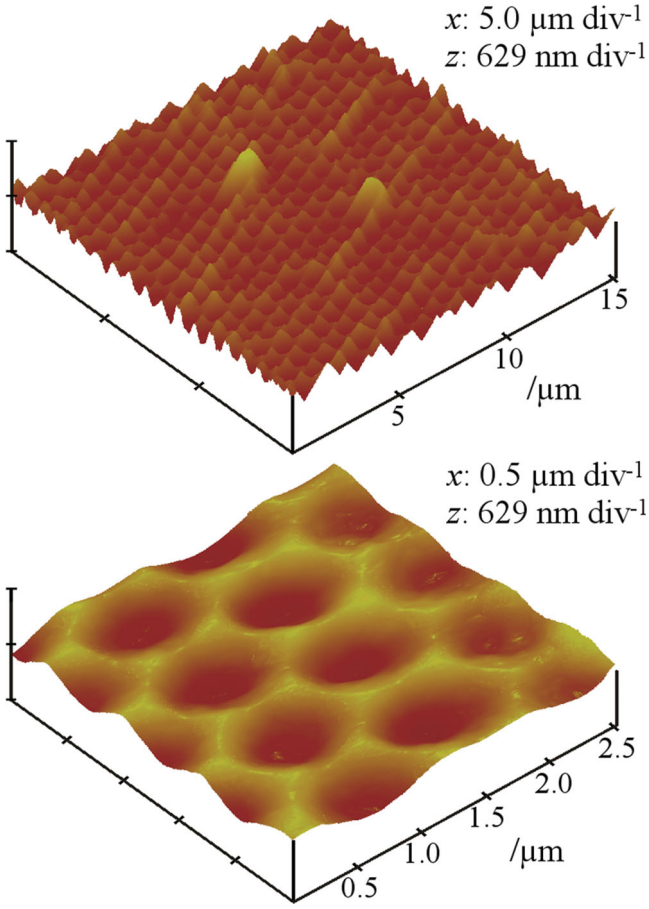

Figure 2. AFM 3D surface reconstructions of the nanopatterned elastomer at two different magnifications. These images demonstrate the successful imprinting of the nanobowls in the PDDC-HD surface.

Tailoring of materials towards the development of thermo-optical systems has attracted considerable interest from the photonics community. On one side, materials without SME have been investigated for thermochromic effects, e.g., the fabrication of inverse opals with demonstrated stopgap dependence on temperature.[30] A more recent work described novel elastomeric crystalline films with triple stimuli response to strain, light and temperature.[31] On the other side, the full advantages of SME are starting to be explored in the design of photonic devices. Davies et al. reported on a chiral-nematic polymer network presenting SME applied into manufacturing an optical temperature sensor, which changed color as the original form of the material was restored above a certain temperature threshold.[32] The SME was also the driving mechanism that enabled Xie and co-workers to develop metallic wrinkle membranes exhibiting structural color.[33,34] They demonstrated a correlation between the pitch of the wrinkles and the strain applied to the polymeric substrate. Besides these findings, Rogers et al. reported on the exploration of SMPs towards the fabrication of micro-optical devices or PCs with reversible but programmable characteristics.[35] By using interference lithography, Yang and colleagues developed membranes with programmable color switching.[36] In comparison to this previous work, our strategy for the fabrication of SME photonic nanostructures presents important advantages due to the use of colloidal crystals as templates. Since these are fabricated with monodisperse particles which are available in a wide range of diameters, an increased control over the final structure and lattice parameter could be achieved. Further, our method is straightforward and does not require complex or expensive equipment.

Light diffraction was used for systematically studying the possibility of programing the sample towards the development of a thermoresponsive optical grating with shape-memory. This was achieved by observing the diffraction figure projected on a screen positioned in the far-field. First, the angle of diffraction (θ_d) was measured for the sample at its initial state. The obtained results and their comparison with the theoretical model (SI) are presented in Table S1. As can be appreciated, the agreement is excellent. We next explored how elongation affected the PC imprinted in the elastomer. A single iteration of the protocol followed is presented in Figure 1b. Diffraction

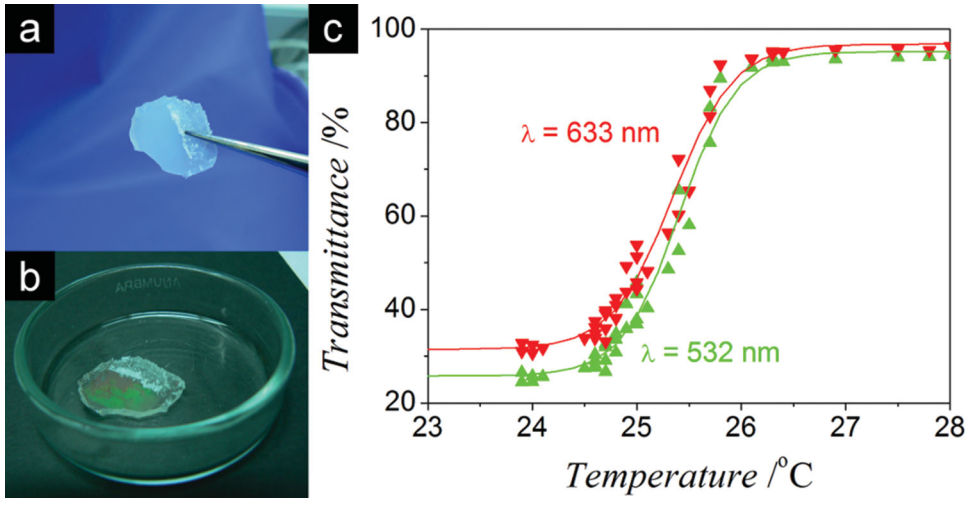

Figure 3. Visual aspect of the surface-nanopatterned PDDC-HD elastomer at room temperature (a) and above T_{trans} (b). Temperature dependence of the total optical transmittance of the sample, for $\lambda = 532$ and 633 nm, exhibiting the change in transparency characteristic of the transition (c).

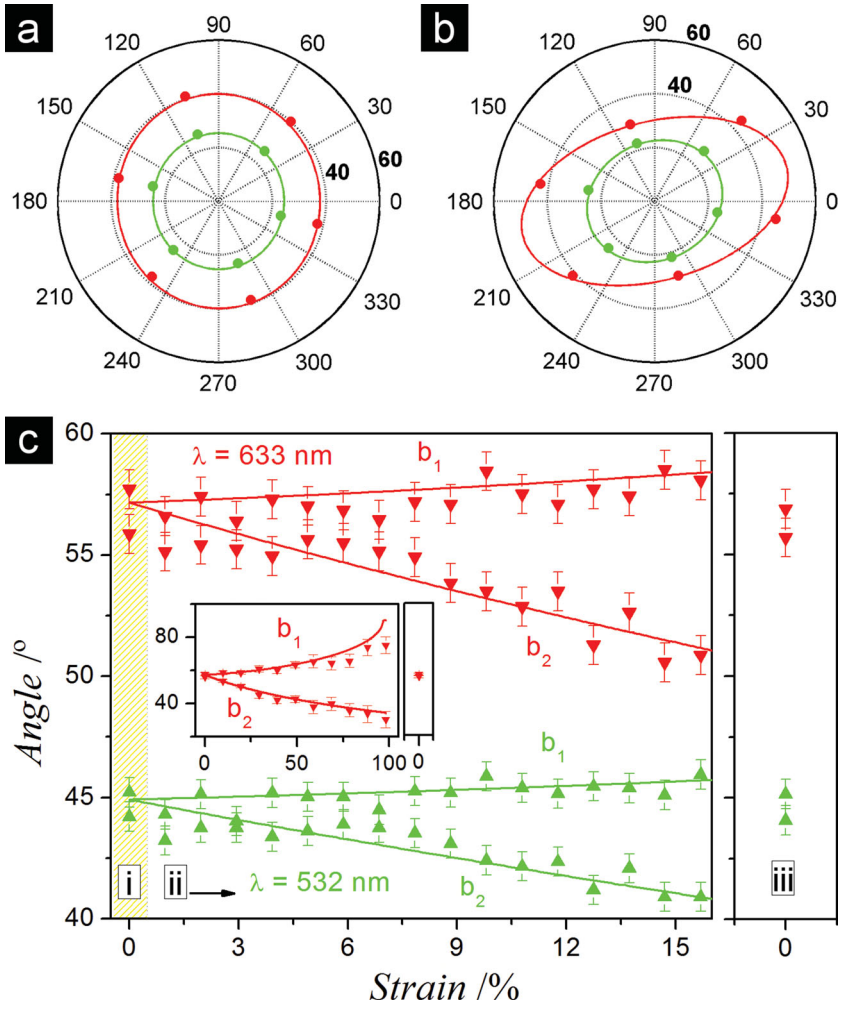

Figure 4. Representative polar plots exhibiting the experimental points coordinates of a diffraction figure from nanopatterned PDDC-HD in the initial state (a) and after fixing a strain of 15% (b) for two wavelengths: $\lambda = 532$ (green) and 633 nm (red). Experimental (triangles) and theoretical (solid lines) behaviors of the diffraction angles along the two principal symmetry directions ($\vec{b}_1$ and $\vec{b}_2$) as a function of the strain imposed to the sample (c). The inset exhibits the complete range up to 100% of strain. Plot on the right (iii) corresponds to the angles measured after re-heating the polymer and recovering its initial shape.

images were collected in the cycle steps labelled as i, ii and iii – some key examples are provided in Figure S4. The process was continued by successively increasing the applied strain while monitoring the diffraction angles along the two symmetry directions ($\vec{b}_1$ and $\vec{b}_2$) of the reciprocal space (**Figure 4**). When the sample was stretched and cooled below T_{trans}, the temporary shape was fixed and thus the lattice parameter increased (decreased) along $\vec{b}_1$ ($\vec{b}_2$ by Poisson effect). These changes in the periodicity of the grating directly affected the diffraction angles and, therefore, the diffraction figure gradually deformed from a circumference to an ellipse as clearly exhibited in Figure 4a and b, respectively. This effect can be compared with the control of plasmonic resonances in stretched hexagonal lattices used for fabricating elliptical gold rings.[37] The behavior of the diffraction angles as a function of the applied strain is presented in Figure 4c, along with the theoretical model discussed in detail in the SI. Strain was increased up to 100% (with greater precision for small strains) while monitoring the angles at $\lambda = 532$ nm or $\lambda = 633$ nm. Good agreement was found between experimental data and theoretical predictions up to strains of 100%, thus confirming that it was possible to fix the lattice parameter of the 2D PC in the predefined way. Nevertheless, the concordance was slightly worse above 60% of strain possibly due to two contributing factors. On the one hand, the deformation got increasingly inhomogeneous along the sample, being more intense near the sustaining clamps. On the other hand, the diffraction spots projected on the screen gradually deformed into line segments implying a worse defined θ_d. In any case, as exhibited in the right plot of Figure 4c, the original diffraction angles were entirely restored after heating the sample at the end of the process, which demonstrates the SME affecting the 2D grating. It is worth noting that the data plotted correspond to a single piece of polymer and that each data point entails a heat-stretch-cool-relax cycle followed by a heat-relax cycle, setting a cyclability indication. In this particular study, up to 35 cycles were achieved with a representative sample. However, a modest cyclability is expected for this type of polymers as higher temperatures impact on polymer cross-linking and gradually eliminate the shape-memory properties of the material while increasing its stiffness.

The second test to ascertain programmable features of the photonic nanostructure imprinted in the PDDC-HD polymer was to study if it could be erased and later recovered by using its SME. This hypothesis was supported by previous work on SME at the nanoscale.[16] The procedure was implemented as depicted in Figure 1c. Accordingly, the sample was compressed between two hydrophobic surfaces of polypropylene. The thickness reduction of the elastomeric piece, after fixing the temporary shape and releasing the applied stress, was on the order of 50%. The morphology of the PDDC-HD elastomer in the three states labelled as i, ii and iii was characterized by AFM, scanning electron microscopy (SEM) and optical diffraction measurements (**Figure 5**). As expected, the obtained pattern profile was very similar for states i and iii, contrarily to that obtained for state ii (Figure 5a). The surface roughness in state ii decreased in comparison to i and iii (**Table 1**), in agreement with its much smoother aspect observed by SEM (Figure 5b). In ii, the pattern might still be intuited, although with a significant decrease of contrast. Finally, diffraction images were collected in order to study how the described behavior affected the optical properties of the PDDC-HD-based PC. As

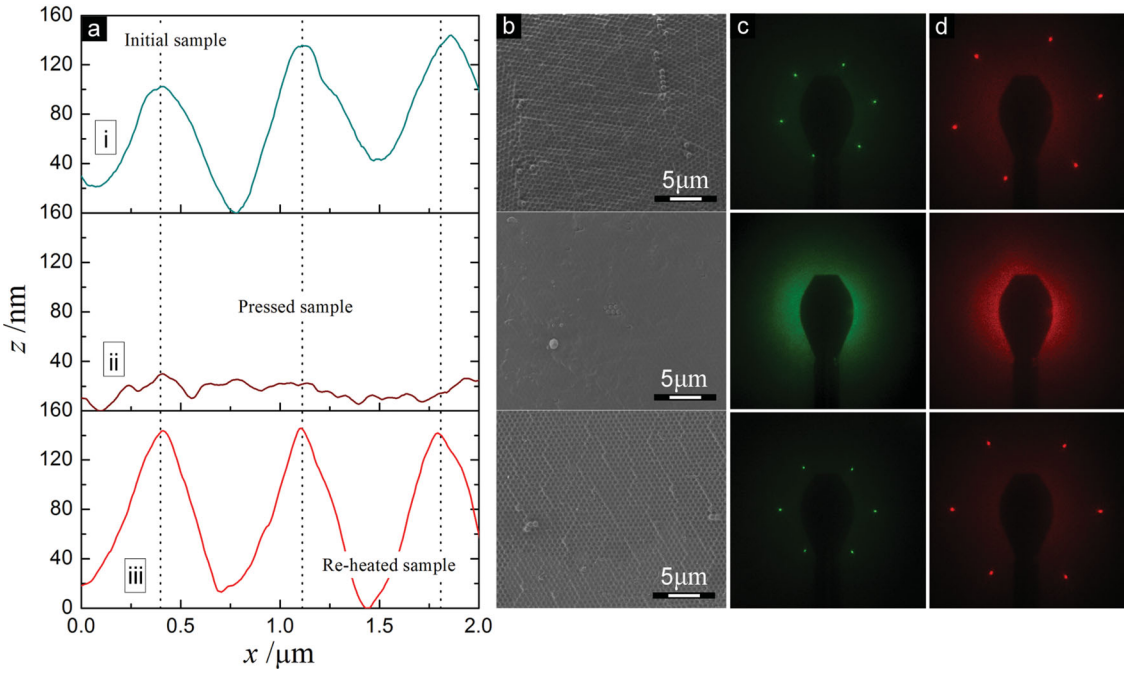

Figure 5. Horizontal profiles as measured by AFM of the initial sample (i), after compression and nanopattern erasing (ii) and after shape recovery (iii) (a). Similar characterization using SEM (b). Diffraction images of the PDDC-HD sample in the referred states for two wavelengths: $\lambda = 532$ and 633 nm (c and d, respectively).

observed in Figure 5c, hexagonal patterns were obtained and reproduced along the entire sample area in states i and iii. On the contrary, for state ii, it was impossible to observe any diffraction image while scanning through the whole surface. We hypothesize that, although the nanopattern was not entirely erased by compression (see results from SEM analysis), the periodic part of the modulation became comparable to, or smaller than, the random part so that light scattering was essentially insensitive to it.

The multifunctional nature of PDDC-HD is confirmed by several interesting features. It is elastomeric, biocompatible, biodegradable and also presents SME and drug releasing capabilities. In the present work, we further expanded this spectrum of functionalities. It was shown that, by using a simple procedure based in replica molding, it was possible to engrave a hexagonal nanostructured pattern from a colloidal crystal template in the surface of the PDDC-HD elastomer. By doing so, we demonstrated the applicability of the reported system in the achievement of active optical elements with thermoresponsive shape-memory characteristics. Two proofs of concept were reported herein, representing advances in both SMPs and photonics fields. Firstly, we showed that the lattice parameter of the 2D grating was programmable and dependent of the strain imposed to the polymer. Secondly, it was feasible to transitorily erase the surface nanopattern from the optical point of view. In both cases, the characteristics of the original structure were entirely recovered by simply heating the sample above T_{trans}, thus proving the SME affecting the optical properties of the PC and also its read/write capabilities with potential application in emergent technologies. Alternatively, the use of light-induced SME, independent from temperature, might be a valuable asset for future developments in this area. We also envision the present system to have a wide impact, not exclusively in the field of photonics, due to the feasibility of incorporating additional components such as bioactive molecules or nanoparticles into the polymeric network. This fact opens a wide range of opportunities for the combination of different functionalities in these nanostructured PDDC-HD elastomers, thus creating systems with application in biomaterials, nanoelectromechanical devices, self-healing optical elements, or devices with programmable hydrophobicity. To guarantee a long-term usage, for this particular choice of materials, storage in dry conditions at temperatures below 4 °C is recommended in order to preserve polymer cross-linking and avoid its degradation. At the same time, their biodegradability could be especially attractive for the fabrication of disposable devices with application in areas such as biomedicine and biophotonics, when only the temporal presence of the material is pursued.

Table 1. Comparison among the average (R_a), root mean squared (R_{rms}) and maximum (R_{max}) surface roughness of the PDDC-HD sample in states i, ii and iii, as measured by AFM.

State	R_a [nm]	R_{rms} [nm]	R_{max} [nm]
i	52.8	68.4	774.8
ii	7.1	9.6	71.1
iii	54.4	68.0	631.3

Experimental Section

Detailed information about the experimental procedures is included in the Supporting Information.

Chemicals: All chemicals were purchased from Sigma-Aldrich and used as received unless otherwise indicated. Colloidal spherical particles of PS with polydispersity of 3% were purchased from Thermo Scientific.

Fabrication of the Monolayers: The monolayers of PS spheres were grown according to a previously reported method.[38] A wedge shape cell was used to confine the colloid and allow solvent evaporation in controlled conditions.

Synthesis of the Elastomer: Elastomer synthesis was performed following the general procedure previously described.[26] To create the surface relief grating on the elastomer, the liquid pre-polymer solution was placed on top of a monolayer of PS spheres of different diameters (either 200 or 870 nm) and allowed post-polymerizing at 90 °C for 12 h (for 2 mm-thick samples). After that time, the cross-linked elastomer (PDDC-HD polymer) was removed from the sphere monolayer by carefully peeling it off when still warm.

Chemical, Thermal and Optical Characterization: ^{1}H-NMR spectrum of the pre-polymer solution was recorded at room temperature by using a Bruker spectrometer DRX-500 at 500 MHz. The mol ratio of DD to citric acid was confirmed as 1.5, according to the theoretical value (mol ratio 3:2, respectively) and corroborating the dominance of hydroxyl versus carboxyl groups in these polymers. Details for the chemical shifts of the different groups are included in SI (Figure S7). The degree of post-polymerization in the resulting cross-linked PDDC-HD was evaluated by calculating the molecular weight between cross-links (M_c) through swelling studies in dimethylsulfoxide.[39] mDSC studies were performed by using a Discovery DSC Calorimeter (TA Instruments). Briefly, samples were cooled to –60 °C, held for 5 min and then ramped from –60 °C to 75 °C at a rate of 2 °C min^{-1} (modulation amplitude ±2 °C and frequency 60 s^{-1}) (Figure S8). Total transmission of the PDDC-HD sample was collected from 90 °C to 23 °C with an integrating sphere fiber-coupled to an Ocean 2000 compact spectrometer. The temperature was monitored in parallel with a thermocamera Fluke Ti10.

Thermomechanical Characterization: The complex Young modulus (viscoelastic behaviour) of the PDDC-HD elastomer was measured from –30 to 50 °C at a rate of 2 °C min^{-1} at 5 Hz in a triple point bending configuration by using a Dynamic Mechanic Analyzer DMA 7e (Perkin Elmer). The first heating run of the DMA spectrum of a representative sample is presented in Figure S9.

Surface Grating Characterization: The surface nanotopography of the PDDC-HD samples was first characterized at room temperature by using an AFM multimode Nanoscope III A (Bruker) with a FESP tip working in tapping mode. Additionally, the nanometric grating was characterized by SEM. Samples were mounted on stubs with carbon tape and visualized in a FEI NovaNano SEM 230 microscope. Finally, diffraction patterns were acquired in a home-built setup extensively described in SI.

Supporting Information

Supporting Information is available from the Wiley Online Library or from the author.

Acknowledgements

This work was partially supported by EU FP7 NoE Nanophotonics4Energy grant No. 248855, the Spanish MICINN project MAT2012–31659 (SAMAP), and *Comunidad de Madrid* S2009/MAT-1756 (PHAMA) program. The authors thank Dr. Francisco del Monte (ICMM-CSIC) for scientific support and fruitful discussions, Dr. María José de la Mata (Servicio Interdepartamental de Investigación, Universidad Autónoma de Madrid, UAM) for assistance with mDSC studies, Dr. Ricardo Jiménez (ICMM-CSIC) for his technical support in thermomechanical characterization studies and Dr. Daniel Jaque (*UAM*) for support with the thermocamera. A.E. was supported by the FPI Ph.D. program from the MICINN. M.C.S. acknowledges MINECO for a *Juan de la Cierva* fellowship.

Received: December 22, 2013
Revised: February 20, 2014
Published online: March 19, 2014

[1] L. C. Chang, T. A. Read, *Trans. AIME* **1951**, *189*, 47.
[2] B. K. Kim, S. Y. Lee, M. Xu, *Polymer* **1996**, *37*, 5781.
[3] Y. Osada, A. Matsuda, *Nature* **1995**, *376*, 219.
[4] M. Behl, A. Lendlein, *Mater. Today* **2007**, *10*, 20.
[5] I. Bellin, S. Kelch, R. Langer, A. Lendlein, *Proc. Natl. Acad. Sci. USA* **2006**, *103*, 18043.
[6] J. W. Cho, J. W. Kim, Y. C. Jung, N. S. Goo, *Macromol. Rapid Comm.* **2005**, *26*, 412.
[7] T. Weigel, R. Mohr, A. Lendlein, *Smart Mater. Struc.* **2009**, *18*, 025011.
[8] A. Lendlein, H. Y. Jiang, O. Jünger, R. Langer, *Nature* **2005**, *434*, 879.
[9] H. Y. Jiang, S. Kelch, A. Lendlein, *Adv. Mater.* **2006**, *18*, 1471.
[10] R. Yoshida, K. Uchida, Y. Kaneko, K. Sakai, A. Kikuchi, Y. Sakurai, T. Okano, *Nature* **1995**, *374*, 240.
[11] A. Lendlein, R. Langer, *Science* **2002**, *296*, 1673.
[12] M. Behl, M. Y. Razzaq, A. Lendlein, *Adv. Mater.* **2010**, *22*, 3388.
[13] A. Lendlein, V. P. Shastri, *Adv. Mater.* **2010**, *22*, 3344.
[14] J. Hu, *Shape Memory Polymers and Textiles*, Woodhead Publishing Limited, Cambridge, UK **2007**.
[15] W. M. Huang, C. W. Lee, H. P. Teo, *J. Intel. Mater. Syst. Str.* **2006**, *17*, 753.
[16] T. Altebaeumer, B. Gotsmann, H. Pozidis, A. Knoll, U. Duerig, *Nano. Lett.* **2008**, *8*, 4398.
[17] J. L. Wilbur, R. J. Jackman, G. M. Whitesides, E. L. Cheung, L. K. Lee, M. G. Pretiss, *Chem. Mater.* **1996**, *8*, 1380.
[18] A. C. Arsenault, T. J. Clark, G. von Freymann, L. Cademartiri, R. Sapienza, J. Bertolotti, E. Vekris, S. Wong, V. Kitaev, I. Manners, R. Z. Wang, S. John, D. Wiersma, G. A. Ozin, *Nat. Mater.* **2006**, *5*, 179.
[19] C. I. Aguirre, E. Reguera, A. Stein, *Adv. Funct. Mat.* **2010**, *20*, 2565.
[20] B. Viel, T. Ruhl, G. P. Hellmann, *Chem. Mater.* **2007**, *19*, 5673.
[21] J. M. Jethmalani, W. T. Ford, *Chem. Mater.* **1996**, *8*, 2138.
[22] J. H. Jang, C. K. Ullal, T. Gorishnyy, V. V. Tsukruk, E. L. Thomas, *Nano Lett.* **2006**, *6*, 740.
[23] M. E. Calvo, H. Míguez, *Chem. Mater.* **2010**, *22*, 3909.
[24] J. Liang, L. Li, X. Niu, Z. Yu, Q. Pei, *Nat. Photonics* **2013**, *7*, 3.
[25] J. Yang, A. R. Webb, G. A. Ameer, *Adv. Mater.* **2004**, *16*, 511.
[26] M. C. Serrano, L. Carbajal, G. Ameer, *Adv. Mater.* **2011**, *23*, 2211.
[27] Y. Xia, G. M. Whitesides, *Angew. Chem. Int. Ed.* **1998**, *37*, 550.
[28] H. J. Nam, D. Jung, G. R. Yi, H. Choi, *Langmuir* **2006**, *22*, 7358.
[29] D. Losic, J. G. Mitchell, R. Lal, N. H. Voelcker, *Adv. Funct. Mater.* **2007**, *17*, 2439.
[30] G. Wu, Y. Jiang, D. Xu, H. Tang, X. Liang, G. Li, *Langmuir* **2011**, *27*, 1505.
[31] C. G. Schäfer, M. Gallei, J. Zahn, J. Engelhardt, G. Hellmann, M. Rehahn, *Chem. Mater.* **2013**, *25*, 2309.
[32] D. Davies, A. R. Vaccaro, S. M. Morris, N. Herzer, A. Schenning, C. Bastiaansen, *Adv. Funct. Mater.* **2013**, *23*, 2723
[33] T. Xie, X. Xiao, J. Li, R. Wang, *Adv. Mater.* **2010**, *22*, 4390.
[34] J. Li, Y. An, R. Huang, H. Jiang, T. Xie, *ACS Appl. Mater. Interfaces* **2012**, *4*, 598.
[35] H. Xu, C. Yu, S. Wang, V. Malyarchuk, T. Xie, J. Rogers, *Adv. Funct. Mater.* **2013**, *23*, 3299.
[36] L. Li, J. Shim, J. Deng, J. Overvelde, X. Zhu, K. Bertoldi, S. Yang, *Soft Matter* **2012**, *8*, 10322.
[37] Y. Cai, Y. Li, P. Nordlander, P. S. Cremer, *Nano Lett.* **2012**, *12*, 4881.
[38] A. Espinha, M. Ibisate, J. Galisteo-López, A. Blanco, C. López, *Langmuir* **2012**, *28*, 13172.
[39] A. R. Webb, J. Yang, G. A. Ameer, *J. Polym. Sci., Part A: Polym. Chem.* **2008**, *46*, 1318.